

Transient Heat Transfer

Unsteady Conduction and Natural Convection

Group Members:

Alciades Velasquez: Lead Author, Title Page, Theory, Uncertainty Analysis for Conduction Part, References

Corey Mitchel: Introduction, Experimental Apparatus and Instrumentation, Experimental Procedure

Loren Faire: Presentation of Convection Results, Analysis and Discussion of Convection Results, Conclusions and Recommendations of Convection Part, Appendices

Santhana Balaji: Presentation of Conduction Results, Analysis and Discussion of Conduction Results, Conclusions and Recommendations of Conduction Part, Uncertainty Analysis for Conduction Part.

Transient Heat Transfer

Unsteady Conduction and Natural Convection

Group Members

Alciades Velasquez
Corey Mitchel
Loren Faire
Santhana Balaji

Experiment Execution: October, 20, 2008

Report Submission: November, 09, 2008

Abstract:

The dimensionless Nu and Gr were calculated from experimental results for an aluminum plate at a horizontal and a vertical convective heat transfer configuration. Similarly, the dimensionless Fo and Bi numbers were calculated to reconstruct the Heisler charts for different shapes and materials for their conduction on a hot water bath. The resulting numbers were then compared with theory. The convective heat transfer results show that heat was transferred more efficiently under the vertical configuration. The Nu and Gr numbers obtained agreed with expected theoretical values and showed a logarithmic relationship to each other. The Heisler charts were successfully and accurately reproduced when compared to theory. The Fo and Bi numbers were slightly off from expected values from theory, but as observed on the Heisler charts, their relationship was correctly maintained.

Contents

List of Figures and Tables	5
Introduction	6
Theory and Background	7
Convection	7
Conduction	9
Experimental Apparatus and Instrumentation	12
Conduction	12
Convection	13
Experimental Procedure	14
Conduction	14
Convection	14
Uncertainty Analysis	15
Conduction	15
Convection	15
Presentation of Results	17
Conduction	17
Brass Slab	18
Stainless Steel Slab	19
Small Brass Cylinder	20
Large Brass Cylinder	21
Brass Sphere	22
Convection	23
Analysis of Results	25
Conduction	25
Convection	26
Conclusions and Recommendations	28
References	29
Appendices	30
Appendix I : Planning Sheet	30
Appendix II: Vertical Natural Convection Sample Data	35
Appendix III: Horizontal Natural Convection Sample Data	36

Appendix IV: Steel Slab Sample Data	37
Appendix V: Brass Slab Sample Data.....	38
Appendix VI: Brass Sphere Sample Data	39
Appendix VII: Small Brass Cylinder Sample Data	40
Appendix VIII: Large Brass Cylinder Sample Data	41
Appendix IX: Sample Calculations	42

List of Figures and Tables

<i>Figure 1. Slab of Thickness $2L$</i>	<i>9</i>
<i>Figure 2. Heisler Chart for a Slab of Thickness $2L$</i>	<i>11</i>
<i>Figure 3. Conduction Experiment Samples Schematic and Dimensions</i>	<i>12</i>
<i>Figure 4. Reconstructed Heisler Chart for the Brass Slab</i>	<i>18</i>
<i>Figure 5. Reconstructed Heisler Chart for the Staintess Steel Slab.....</i>	<i>19</i>
<i>Figure 6. Reconstructed Heisler Chart for the Small Brass Cylinder</i>	<i>20</i>
<i>Figure 7. Reconstructed Heisler chart for the Large Brass Cylinder</i>	<i>21</i>
<i>Figure 12. Reconstructed Heisler chart for the Brass Sphere</i>	<i>22</i>
<i>Figure 8. Temperatures of Horizontal Plate for 30 Minute Cooling Period</i>	<i>23</i>
<i>Figure 9. Temperatures of Vertical Plate for 30 Minute Cooling Period.....</i>	<i>23</i>
<i>Figure 10. Nu Vs Gr Vertical</i>	<i>24</i>
<i>Figure 11. Nu Vs Gr Horizontal.....</i>	<i>25</i>
 <i>Table 1. Conduction Calculation Parameters</i>	 <i>17</i>
<i>Table 2. Empirical Quantities Based on T_{film} Values.</i>	<i>24</i>

Introduction

When dealing with problems and applications involving heat transfer, there are three main methods by which heat can move to and from an object. These three methods of heat transfer are conduction, convection, and radiation. The most common and predominant forms of heat transfer on earth are conduction and convection, while radiation predominates in space applications and some other special cases—especially at very high temperatures. Therefore it is important for mechanical engineers to have a thorough understanding of conductive and convective heat transfer. The objective of this experiment is to analyze the speed of heat transfer for both conduction and convection.

For conduction to happen, two objects must be in physical contact with one another so that heat can be transferred from the hot object to the cooler one. Conduction is accomplished by the interaction of molecules between two solid materials and usually takes place faster than the other two methods due to a large heat transfer coefficient between two surfaces in contact. This experiment will test conduction for different shapes of brass and steel specimens in a hot water bath.

For convection to happen, a moving fluid at a different temperature—whether liquid or gas—must be passing over the surface of the material. Convection takes place by both random molecular motion at the materials surface and the bulk movement of the fluid across the surface moving heat away from the materials surface and being replaced with cooler air. Convection due to the natural motion of air across a surface takes a much longer time than conduction due to a smaller heat transfer coefficient. This experiment will test the natural convection for an aluminum plate using air as a fluid. The objectives for this experiment include finding the Biot, Nusselt, and Grashoff numbers, construct a Heisler chart and finally compute the radiative and convective heat transfer coefficients.

Theory and Background

Convection

Convective heat transfer is produced when an object is heated or cooled by the motion of a fluid around it. This mode of heat transfer is comprised of two mechanisms: energy transfer due to diffusion and energy transfer due to the bulk motion of the fluid ^[2]. Convection transfer can be classified according to the nature of the flow. When the fluid motion is caused by external means, it is referred to as *forced convection* ^[2]. Fluid motion can also be caused by the temperature difference between an object and the surrounding environment, due to changes in the density of the fluid caused by the heat, and this is referred to as *free convection* ^[1].

Regardless of the type of convection, the convective heat flux (heat transfer per unit area), q'' is given by equation 1 shown below ^[1].

$$q'' = h(T_s - T_\infty) \dots\dots\dots 1$$

Where h is the heat transfer coefficient, T_s is the surface temperature, and T_∞ is the temperature of the surrounding fluid. The heat transfer coefficient, h can be non-dimensionalized, thus yielding what is referred to as the *Nusselt number* (Nu) as shown below by equation 2 ^[1].

$$Nu = hL/k \dots\dots\dots 2$$

Where L is the characteristic length of the system, and k is the thermal conductivity of the fluid.

In forced convection, the Nusselt number is usually a function of the Reynolds number. For high speed flows it may also be a function of the Mach number. In free convection, the Nusselt number is usually a function of the *Grashoff number* which can be calculated according to equation 3 ^[1].

$$Gr = \frac{g\beta(T_s - T_\infty)L^3}{\nu^2} \dots\dots\dots 3$$

Because the plate is being tilted along one axis, the width of the plate should be used as the length value for equations 2 and 3.

Where g is the gravitational acceleration, β is the volumetric thermal expansion coefficient, and ν is the kinematic viscosity. In addition to that, β is physically defined by equation 4 ^[1].

$$\beta = -\frac{1}{\rho} \left(\frac{\partial \rho}{\partial T} \right)_p \dots\dots\dots 4$$

However, using the ideal gas law, equation 4 simplifies to equation 5 for ideal gases ^[1].

$$\beta = 1/T \dots\dots\dots 5$$

For equations 2 through 5 the properties k , β , and ν should be calculated based on the film temperature, which is the average of T_s and T_∞ .

For surfaces at high temperatures, radiation heat transfer is a factor. Radiation is emitted by matter at a nonzero temperature and it may be attributed to changes in the electric configuration of the constituent atoms or molecules ^[2]. The radiative heat transfer loss q''_{rad} can be calculated according to equation 6 ^[1].

$$q''_{rad} = \sigma \epsilon (T_s^4 - T_\infty^4) \dots\dots\dots 6$$

Where σ is the Stefan-Boltzmann's constant and ϵ is the emissivity of the surface. With some algebraic manipulation, this becomes a heat transfer coefficient h_{rad} as shown below by equation 7 ^[1].

$$h_{rad} = \sigma \epsilon (T_s^2 + T_\infty^2) (T_s + T_\infty) \dots\dots\dots 7$$

Therefore, the total heat transfer coefficient for the convective part of the experiment is found by adding these together as shown by equation 8 ^[1].

$$h_t = h + h_{rad} \dots\dots\dots 8$$

The experiment uses an aluminum plate, which is heated, and then allowed to cool down. Applying conservation of energy principles, the rate at which heat is lost from the plate can be calculated by equation 9 ^[1].

$$Q'' = Aq'' = Ad\rho_s c_{p,s} \frac{\partial T_s}{\partial t} \dots\dots\dots 9$$

Where Q'' is the total heat loss per unit time, A is the area of the plate, d is the thickness of the plate, ρ_s is the density of the plate, and $c_{p,s}$ is the specific heat of the plate. Combining equations 1, 8, and 9, equation 10 is obtained ^[1].

$$q'' = d\rho_s c_{p,s} \frac{\partial T_s}{\partial t} = h_t (T_s - T_\infty) \dots\dots\dots 10$$

Based on equation 10, if the dimensions, thermal properties, and temperature of the plate as a function of time are known, the total heat transfer coefficient can be calculated. Equations 7 and 8 can then be used to find the convection heat transfer coefficient h ^[1].

Conduction

Conduction is dictated by the transfer of energy from more energetic to less energetic particles within a substance due to the interactions between the particles ^[2]. Unsteady conduction occurs when an object is heated or cooled, such as taking an object in or out of an oven or furnace ^[1].

Let's consider a slab of thickness $2L$ as shown in figure 1 below.

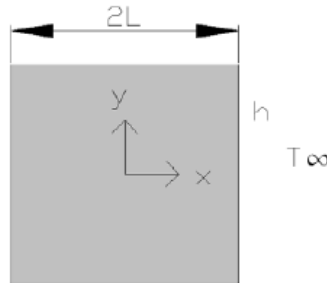


Figure 1. Slab of Thickness $2L$ ^[1]

If the thermal conductivity k_s , density ρ_s , specific heat $c_{p,s}$ of the solid are all constant, and there is no internal heat generation, then the transient conduction reduces to equation 11 ^[1].

$$\frac{\partial^2 T}{\partial x^2} = \frac{1}{\alpha} \frac{\partial T}{\partial t} \dots\dots\dots 11$$

Where α is given by equation 12 ^[1].

$$\alpha = \frac{k_s}{\rho_s c_{p,s}} \dots\dots\dots 12$$

The slab will be at a uniform temperature at the start of this process, so equation 13 is applied ^[1].

$$T(x, t = 0) = T_i \dots\dots\dots 13$$

The temperature will also be symmetric around the center-line of the slab, as demonstrated by equation 14 ^[1].

$$\left. \frac{\partial T}{\partial x} \right|_{x=0} = 0 \quad \dots\dots\dots 14$$

At the edge, where the solid meets the fluid, the heat flux due to conduction must be equal to the heat flux due to convection, yielding equation 15 ^[1].

$$-k_s \left. \frac{\partial T}{\partial x} \right|_{x=0} = h \cdot [T(L, t) - T_\infty] \quad \dots\dots\dots 15$$

These equations can be simplified by using a non-dimensional representation of time known as the Fourier number (Fo) a non-dimensional temperature θ^* , and a non-dimensional quantity known as the Biot number (Bi). The position of the slab can be non-dimensionalized as well using the characteristic length to yield x^* . These quantities are defined by equations 16, 17, 18 and 19 ^[1].

$$Fo = \frac{\alpha t}{L^2} \quad \dots\dots\dots 16$$

$$Bi = \frac{hL}{k_s} \quad \dots\dots\dots 17$$

$$\theta^* = \frac{T - T_\infty}{T_i - T_\infty} \quad \dots\dots\dots 18$$

$$x^* = \frac{x}{L} \quad \dots\dots\dots 19$$

Using the non-dimensional numbers defined above, equations 11, 13, 14, and 15 become equations 20, 21, 22, and 23 ^[1].

$$\frac{\partial^2 \theta^*}{\partial x^{*2}} = \frac{\partial \theta^*}{\partial Fo} \quad \dots\dots\dots 20$$

$$\theta^*(x^*, Fo = 0) = 1 \quad \dots\dots\dots 21$$

$$\left. \frac{\partial \theta^*}{\partial x^*} \right|_{x^*=0} = 0 \quad \dots\dots\dots 22$$

$$-\left. \frac{\partial \theta^*}{\partial x^*} \right|_{x^*=0} = Bi \cdot \theta^*(1, t^*) \quad \dots\dots\dots 23$$

Based on these non-dimensionalizations, two systems with the same Bi number should behave the same. This scaling was used to prepare the Heisler charts, an example of which can be shown below ^[2].

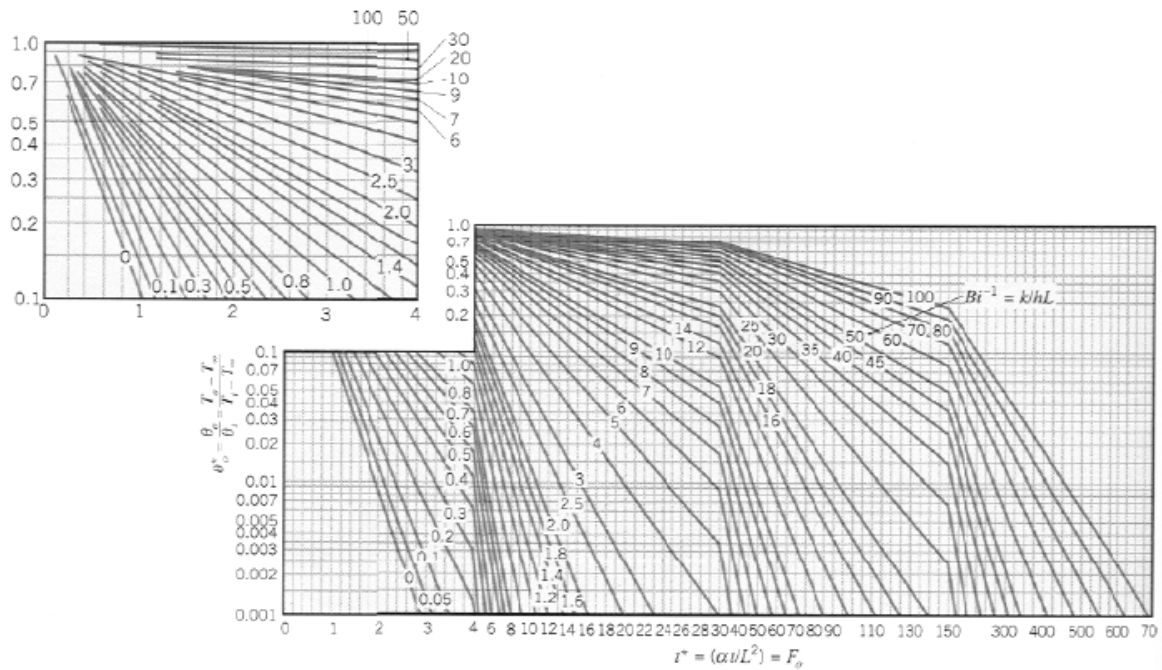


Figure 2. Heisler Chart for a Slab of Thickness $2L$ ^[1]

The Heisler chart can actually be read two ways. If the Biot number is known, the temperature as a function of time can be predicted. Similarly, if the temperature as a function of time is known, then the Biot number, and h , can be extracted.

Experimental Apparatus and Instrumentation

Conduction

Equipment and Apparatus:

1. Armfield HT10X Heat Transfer Service Unit made up of:
 - One insulated water tank used to contain the hot water bath.
 - One electric heating plate located underneath the water tank, used to heat the water in the tank.
 - One gear pump used to circulate the hot water with the purpose of maintaining a uniform temperature across.
 - Rubber hoses connecting the pump to the water tank to circulate the water.

Instrumentation:

1. One thermocouple with a $0.00001\text{ }^{\circ}\text{C}$ resolution was mounted inside the container to measure water temperature.
2. One thermocouple with a $0.00001\text{ }^{\circ}\text{C}$ resolution was internally mounted to the test pieces to measure the internal temperature of the piece.
3. One thermocouple with a $0.00001\text{ }^{\circ}\text{C}$ resolution was rubber banded to the surface of the test pieces to measure each of their the surface temperatures.
4. One A/D Data Logger Unit which was connected to a laptop computer running the Data Acquisition Software.

Tested Equipment:

1. Brass shapes
 - One 45mm diameter sphere
 - One 30mm diameter by 100mm length cylinder
 - One 20mm diameter by 100mm length cylinder
 - One 67x100x15mm slab
2. One 67x100x15mm steel slab

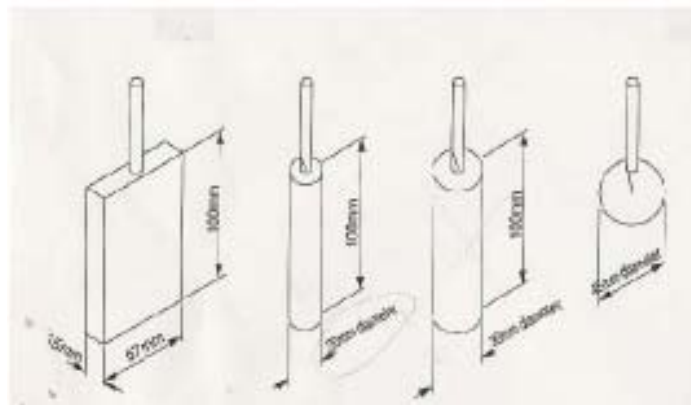


Figure 3. Conduction Experiment Samples Schematic and Dimensions ^[3]

Convection

Equipment and Apparatus:

1. One swivel stand to allow the sample to rotate 360 degrees.
2. One removable burner placed below the swivel stand to heat the aluminum plate.
3. One propane cylinder connected to the removable burner to provide the propane for combustion.
4. A metal wire mesh enclosure was used to safely keep all the testing equipment and apparatus.

Instrumentation:

1. One thermocouple with a 0.0001°C resolution attached to the middle of the sample to measure centerline the temperature.
2. One thermocouple with a 0.0001°C resolution attached to the end of the sample to measure the end temperature.

Tested Equipment:

1. A 9"x18"x0.25" aluminum plate.

Experimental Procedure

Conduction

To begin the conduction experiment, the unit was switched on to begin heating up and circulating the water. While the water was heating, the first shape was hooked up to the mounting cap and a rubber band placed around the specimen to hold the thermocouple to its surface. Once the water temperature had reached 80°C the data started to be recorded. Then the specimen was quickly immersed into the water and the temperatures carefully monitored. After the three temperatures (water, specimen surface, and specimen core) had reached steady state, recording of the data was stopped and the specimen removed from the water. This procedure was repeated for each of the test specimens.

Convection

To begin the convection experiment, the plate was turned upside down, the propane regulator turned on, and the burner orifices lighted with to heat the plate up to 250°C. Once 250°C was reached on the plate, the gas was turned off, the burner unplugged and taken out of the enclosure. The aluminum plate was then turned to a horizontal, upright position and the data recording was started for 1800 seconds. After the 1800 seconds had passed the data was saved and the plate was then heated back up. Once the plate reached 250°C again, the procedure was repeated for cooling of the plate in a vertical position.

Uncertainty Analysis

The uncertainty analysis is a long and iterative process that takes the errors in the measured quantities to determine the uncertainty in the computed quantities. For these experiment all the temperatures represent the measured values. For the conduction experiment, the thermocouples had a resolution of 0.00001°F, while the ones used in the convection experiment had a resolution of 0.0001°F. Aside from the temperatures, the dimensions given for the various shapes also have a resolution value assumed to be 0.01mm for conduction and 1 inch for convection, as this is how they were provided. These quantities were then used to calculate the uncertainties related to these experiments.

To obtain the uncertainty from the accuracy of the instruments a mathematical formula is used to calculate how these individual errors compound to give the net error in a calculation. The equation used for this purpose is equation 24 ^[4].

$$[\varepsilon(F)]^2 = \left[\left(\frac{\partial F}{\partial x_1} \varepsilon(x_1) \right)^2 + \left(\frac{\partial F}{\partial x_2} \varepsilon(x_2) \right)^2 + \dots + \left(\frac{\partial F}{\partial x_i} \varepsilon(x_i) \right)^2 \right] \dots\dots\dots 24$$

Where F is the calculated quantity, ε is the absolute error and x_1 , x_2 , etc are the measured variables.

Conduction

$\varepsilon(\theta) = 0.037 F$ (this was taking into account the variation of the external temperature of the water tank to be +/- 1F)

$\varepsilon(F_o) = 1$ unit (this was at maximum error, with characteristic length (L) assumed to be known to 0.01 mm. *Note: this shows the dramatic effect that a change in the characteristic length would have on the calculations. Therefore, corrosion build-up, imprecise machining or any other factors that could change the characteristic length would have a very large effect on the calculations*)

The other values were either of indeterminable uncertainty such as the values read from a chart, or were taken to be without error (such as the material properties listed in the textbook).

Convection

For the horizontal case, the following uncertainties have been calculated:

$$\varepsilon(h_T) = 1.67e-6 \text{ W}$$

$$\varepsilon(Nu) = 0.251 \text{ units}$$

$\varepsilon (\text{Gr}) = 46785.9$ units (Note: This number is so high due to the fact that the Gr numbers are also very high. However, they represent only a 0.055 percent of the calculated Gr values)

For the vertical case, the following were obtained:

$$\varepsilon (h_T) = 1.685\text{e-}6 \text{ W}$$

$$\varepsilon (\text{Nu}) = 0.0255 \text{ units}$$

$\varepsilon (\text{Gr}) = 49723$ units (Note: This number is so high due to the fact that the Gr numbers are also very high. However, they represent only a 0.055 percent of the calculated Gr values)

Presentation of Results

Conduction

For the transient conduction part of the experiment, the objectives were to measure centerline temperatures as a function of time for the different shapes tested (slabs, cylinders and sphere, both brass and stainless steel) and use those values to reconstruct the Heisler charts for those shapes. From the Heisler charts, the Biot numbers and the heat transfer coefficients were derived.

The Heisler charts were constructed to match precisely with those provided in the Lab manual and the Heat Transfer text ^{[1][2]}– the horizontal axis was a logarithmic axis to the base 10, and the vertical axis was normal scale. The Heisler chart lines were referenced by their point of intersection with the horizontal *Theta centerline* = 0.001 mark. Therefore, the reconstructed lines from this experiment have been shown extrapolated to their 0.001 mark, and the corresponding Fourier number (Fo) was used to derive the Biot (Bi) number. The reconstructed Heisler charts for the different specimens, along with corresponding Biot numbers and h values are shown below. On the Heisler charts, the horizontal axis is the Fourier number (Fo), and vertical axis is the centerline non-dimensional temperature difference (θ). These were calculated by equations 16 and 18 respectively.

In addition, the following parameters were used for the different specimens:

Table 1. Conduction Calculation Parameters ^[2]

Parameter	Value Used
Alpha of Cartridge Brass	33.9 E-6 m ² /s
Alpha of Stainless Steel 302	3.9 E-6 m ² /s
Conductivity (k) of Brass	110.0 W/m.K
'k' of Stainless Steel 302	15.1 W/m.K
Characteristic length (L) for Brass Slab	7.5 mm
L for Stainless Steel Slab	7.5 mm
L for Small Brass Cylinder	10.0 mm
L for Large Brass Cylinder	15.0 mm
L for Brass Sphere	22.5 mm

Brass Slab

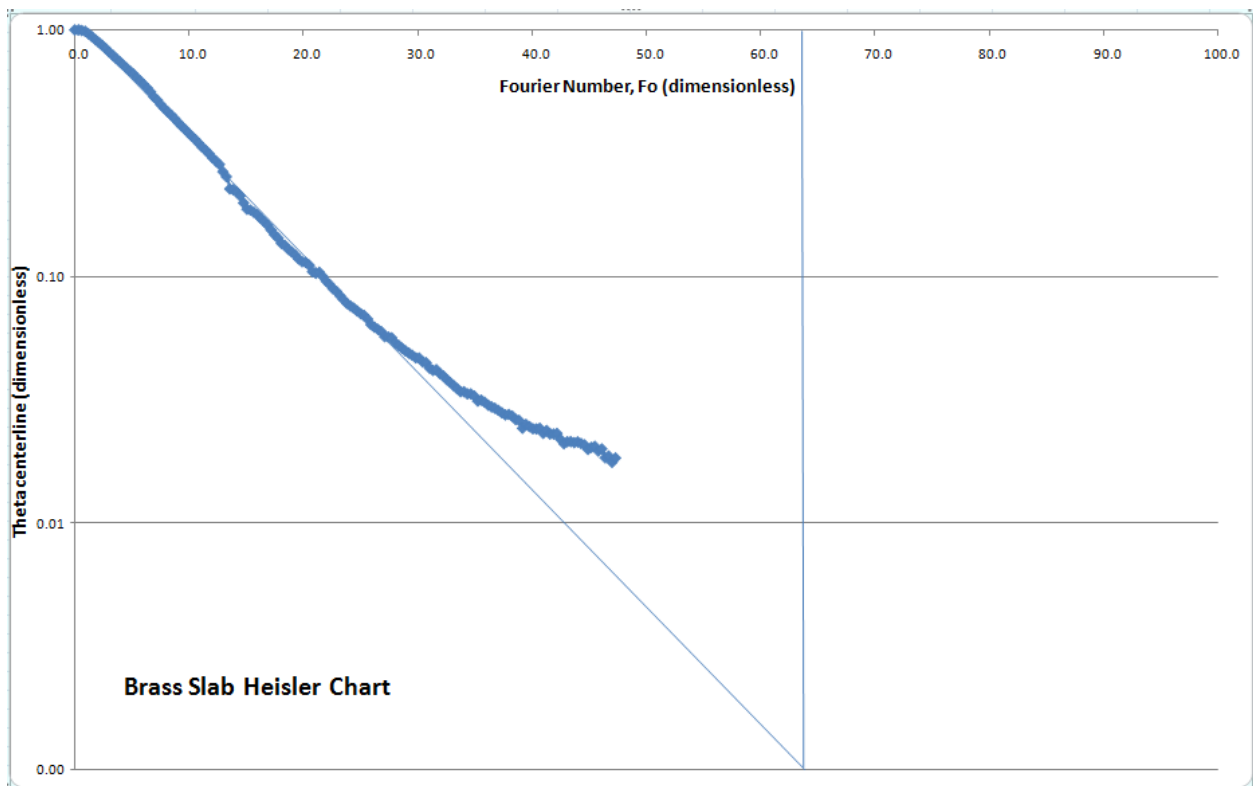


Figure 4. Reconstructed Heisler Chart for the Brass Slab

As mentioned before, the data collected was extrapolated to meet the Theta 0.001 mark, and the corresponding Fourier number was used to calculate the Biot number and the heat transfer coefficient value.

- Biot Number, $Bi = 0.111$ (dimensionless)
- Heat Transfer Coefficient, $h = 1629.63 \frac{W}{m^2 K}$

Stainless Steel Slab

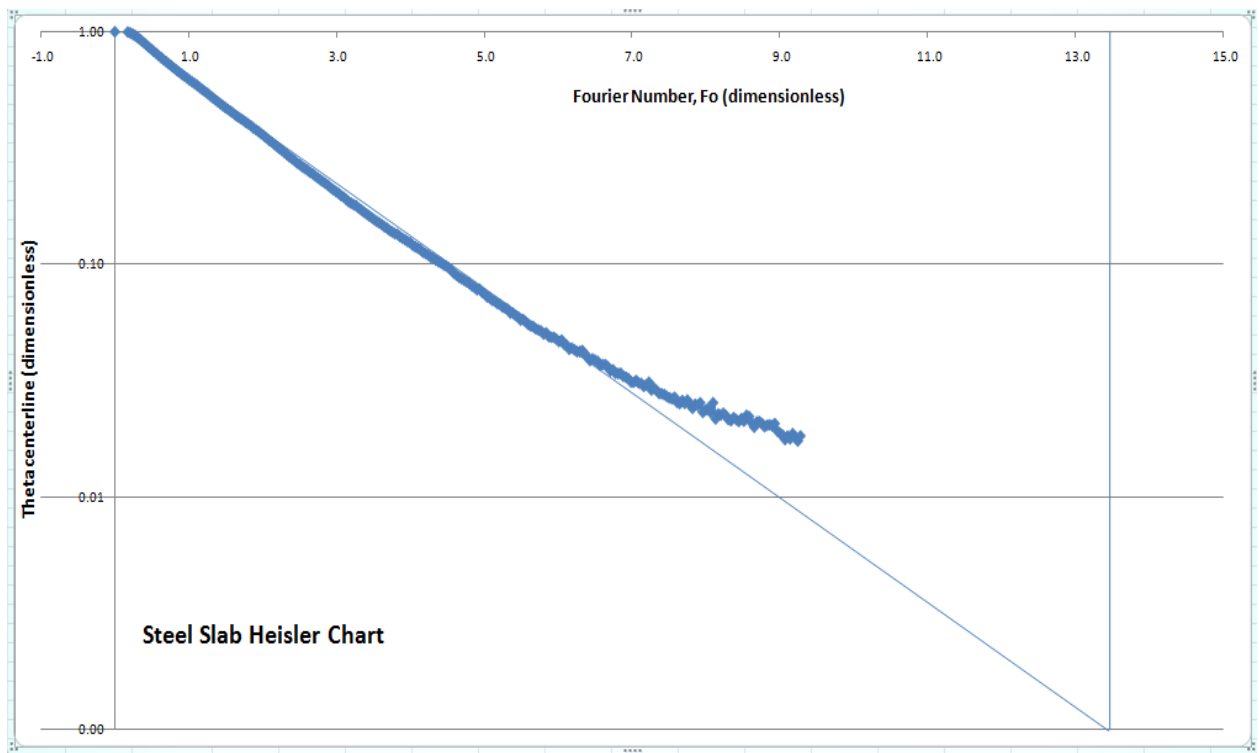


Figure 5. Reconstructed Heisler Chart for the Stainless Steel Slab

- Biot Number, $Bi = 0.606$ (dimensionless)
- Heat Transfer Coefficient, $h = 1220.20 \frac{W}{m^2 K}$

Small Brass Cylinder

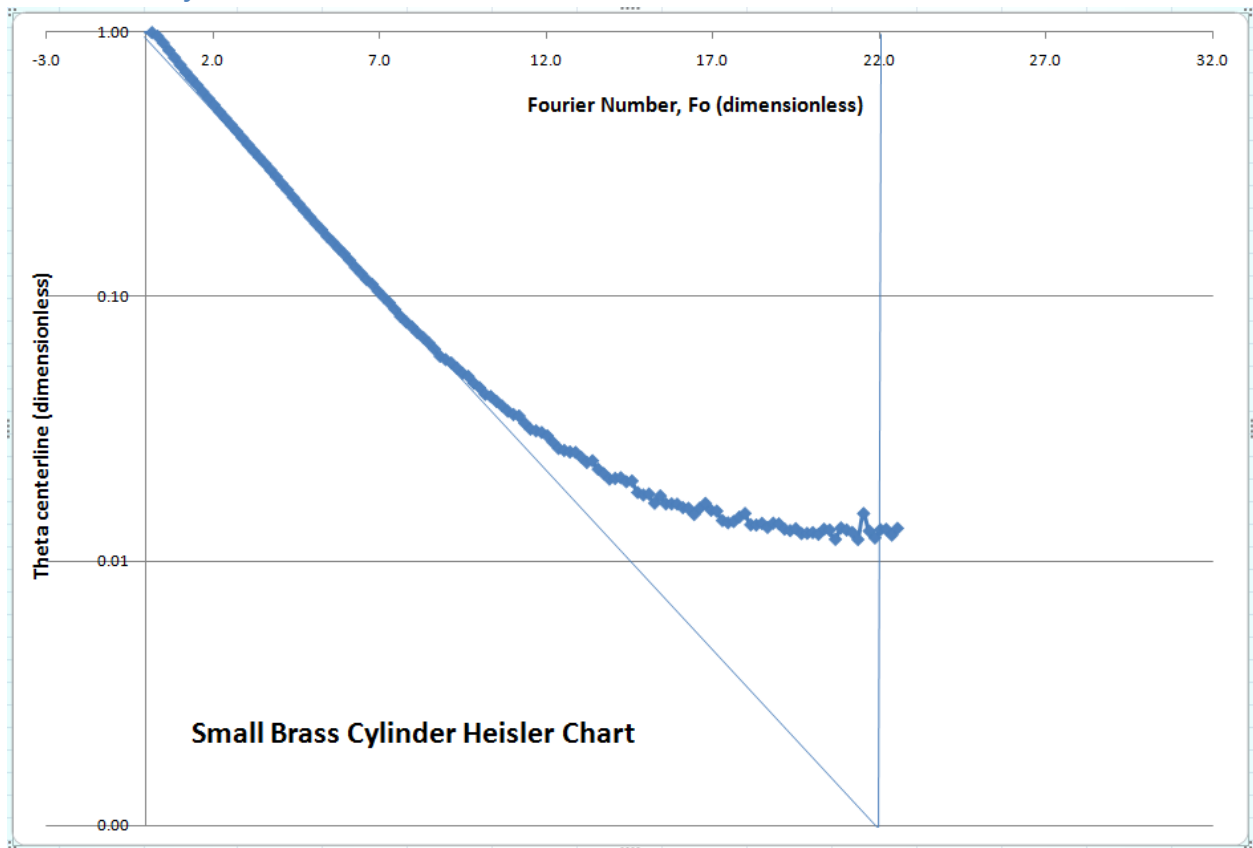


Figure 6. Reconstructed Heisler Chart for the Small Brass Cylinder

- Biot Number, $Bi = 0.167$ (dimensionless)
- Heat Transfer Coefficient, $h = 1833.33 \frac{W}{m^2 K}$

Large Brass Cylinder

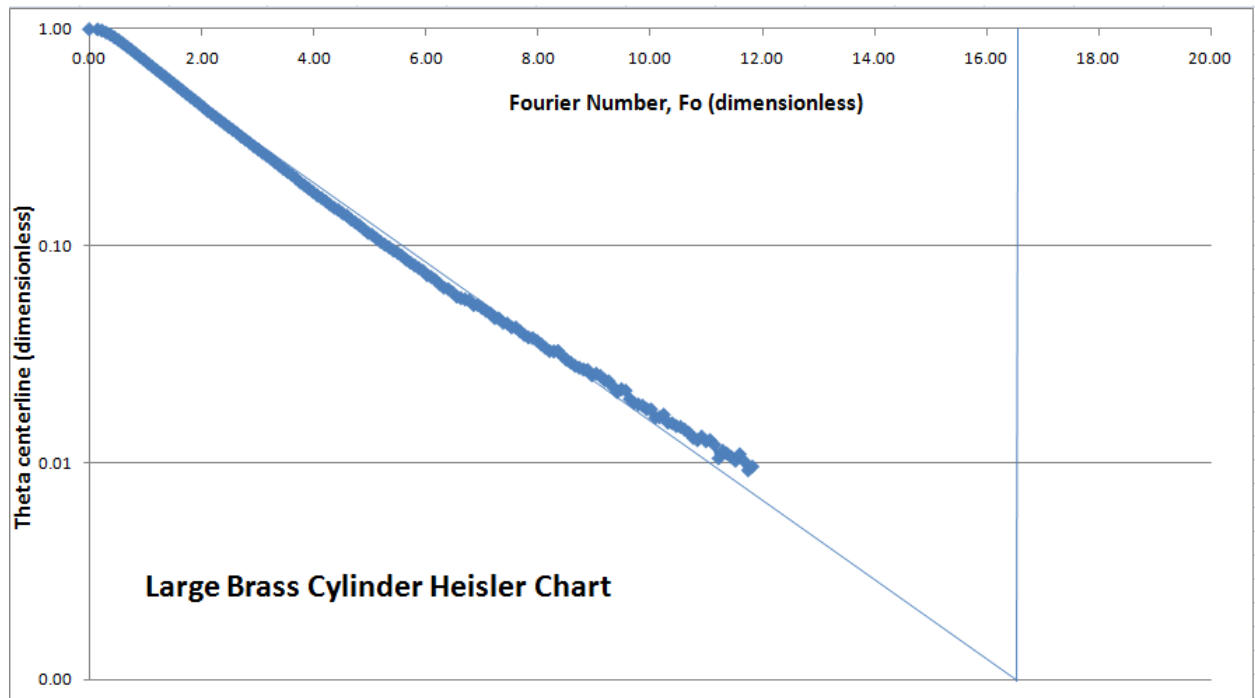


Figure 7. Reconstructed Heisler chart for the Large Brass Cylinder

- Biot Number, $Bi = 0.222$ (dimensionless)
- Heat Transfer Coefficient, $h = 1629.63 \frac{W}{m^2 K}$

Brass Sphere

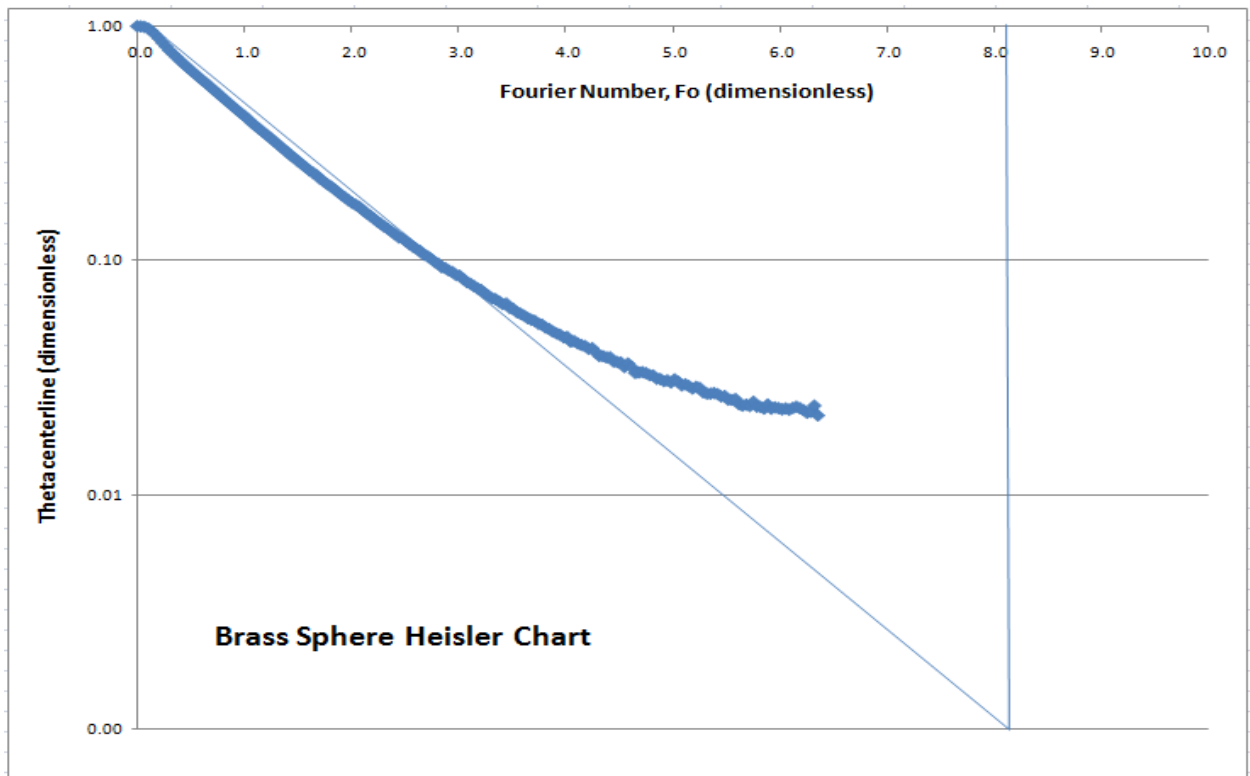


Figure 8. Reconstructed Heisler chart for the Brass Sphere

- Biot Number, $Bi = 0.278$ (dimensionless)
- Heat Transfer Coefficient, $h = 1358.03 \frac{W}{m^2 K}$

Convection

All data points from the free or natural convection portion of the lab were recorded and used to determine the heat transfer behavior of this portion of the experiment. Two configurations: horizontal and vertical were tested and calculated. The initial plots of the temperature distribution from 250 °C to a final temperature for a duration of 30 minutes is shown below for the horizontal case.

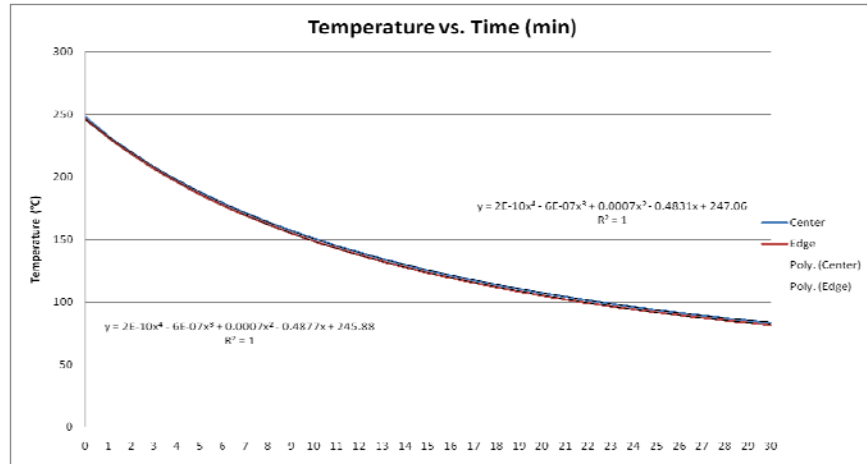


Figure 9. Temperatures of Horizontal Plate for 30 Minute Cooling Period

The equations empirically determined from the data of the temperature as a function of time are:

The resulting plot of the vertical plate temperature distribution is shown below.

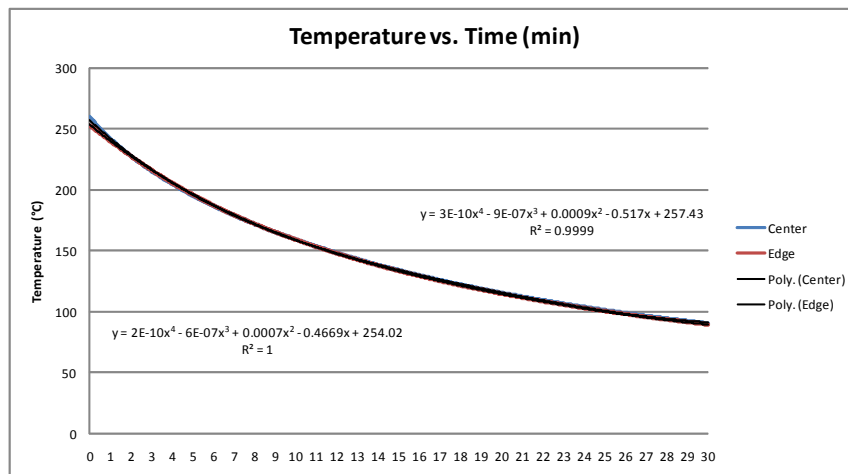


Figure 10. Temperatures of Vertical Plate for 30 Minute Cooling Period

The equations for temperature as a function of time as empirically determined are:

$$T_{edge} = 3 * 10^{-10}t^4 - 9 * 10^{-7}t^3 + .0009t^2 - .517t + 257.43$$

$$T_{center} = 2 * 10^{-10}t^4 - 6 * 10^{-7}t^3 + .0007t^2 - .4669t + 254.02$$

The real value from temperature is that it makes it easier to calculate the heat transferred and analyze the dimensionless numbers associated with heat transfer. The heat rates, transfer coefficients, and total heat transferred are shown in the table below.

Table 2. Empirical Quantities Based on T_{film} Values.

	Convective		Radiative				
	Q (W)	q"(W/m ²)	Q	q"	hc (W/m ² K)	hr	ΔT
Vertical	153.87	1418.00	253.03	2331.77	6.035624	170014680.2	169.27
Horizontal	143.69	1324.16	223.31	2057.83	5.94	161910750.09	164.91

The plots for the Nusselt vs the Grashof plots are shown below and follow the accepted range and slope from wide ranging empirical data.

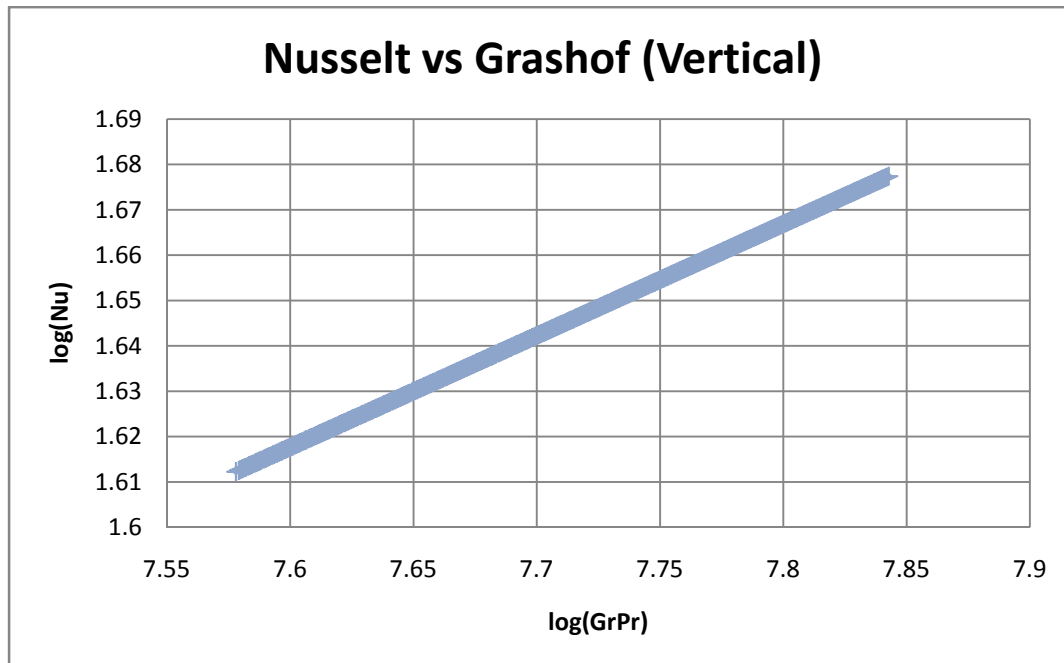


Figure 11. Nu Vs Gr Vertical

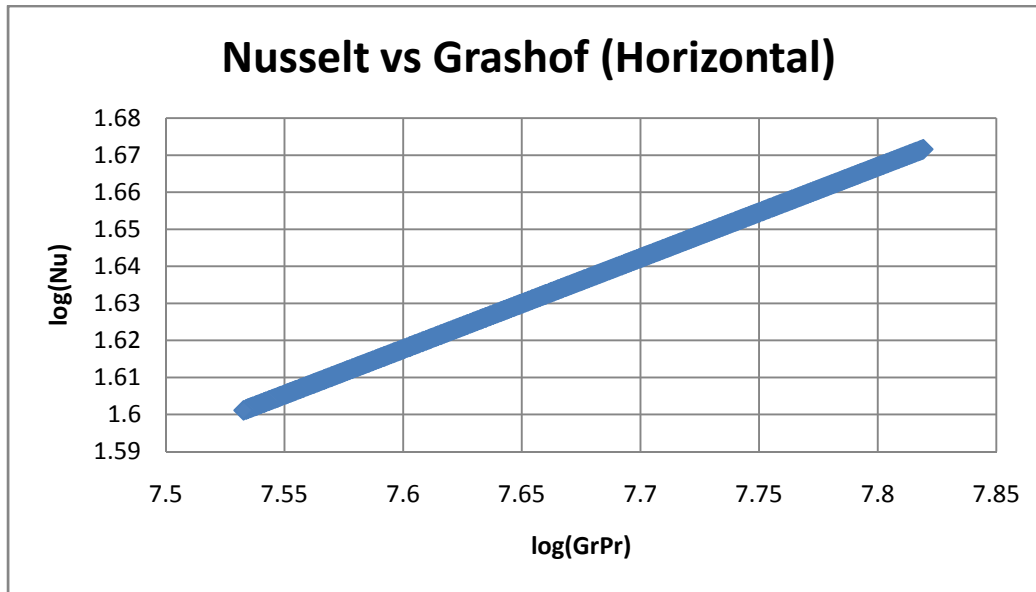


Figure 12. Nu Vs Gr Horizontal

Analysis of Results

Conduction

The results were of good quality for the most part, with the discrepancies and errors due to easily traceable sources. The Heisler charts, when scaled and re-constructed properly, were nearly linear in some cases and in others had predominant linear portions that made the derivations of the Biot numbers easy. The Biot numbers of the different specimens followed all expected trends. The Biot number ($\frac{hL}{k}$) of the brass slab was much smaller than that of the steel slab; and since the heat transfer coefficients and characteristic lengths were nearly the same, the Biot numbers should have been a function of the conductivities only. And from the results it can be seen that Brass, which has a conductivity (k) about six times larger than Stainless steel, has a Biot number about six times smaller than Stainless Steel. This agrees very well with the formula of the Biot number, and is indicative of the good quality of the results. Likewise, the Biot number of the small cylinder is around 1.5 times smaller than the Biot number of the large cylinder, which agrees very well with theory since the characteristic length (L) of the large cylinder is 1.5 times larger than that of the small cylinder. The brass sphere, which had the largest characteristic length of them all (22.5 mm – the larger characteristic length makes heat transfer a slower phenomena) had the largest Biot number also, which again agrees well with theory. While the trends followed were correct, the numbers did not fully numerically match what they ought to have been. These errors magnified as further calculations were performed.

The calculated heat transfer coefficients (h) showed larger inconsistency and discrepancy. The calculated heat transfer coefficients varied from 1220 to 1833.3, with a standard deviation of $240 \frac{W}{m^2 K}$, which is large.

The reasons for errors could be many, and can easily be traced. For one, the external temperature (T_{∞}) of the water bath is assumed to be constant in theory but from the recorded measurements it can be seen that it varies as the water cools down and is heated back up in an effort to keep in constant. This variance would affect the Theta values calculated, and thus affect the Heisler charts. A major reason for errors could be the method of measuring the temperature at the surface of the specimens; the rubber band holding the thermocouple against the surface of the specimen can easily slip. Another reason for the discrepancies might be material related. The brass used was assumed to cartridge brass, and the stainless steel to be Stainless steel 302. If the alloys were of different composition, or if the outside surfaces had built corrosion products, the material properties would change and this would have a significant impact on the calculated values. Another source of errors is the Heisler charts themselves. Small changes in the start and end locations, or the extrapolation line drawn would have very large effects on the calculated values. It must also be mentioned that for the cylinder and slab specimens, the calculations and Heisler charts assume infinite geometries which is only an approximation in this case. Also, in all calculations, one-dimensional heat transfer was assumed while the real nature of heat transfer through the specimens is more complex. Finally, as with any computer read data, the data acquisition methods could be a source of repetitive error if the filtering or the signal conditioning and calibration are not done correctly.

Convection

Initial inspection of figure 8 shows that the edge temperature remains lower than the center for the duration of the cooling time period. This is because of two reasons:

1. The center is heated down the center line due to the burning being along its long axis and the edges “see” less heat transfer to them from both radiation and conduction.
2. Convective and radiative heat transfers are greater at the edges as the thickness allows for three dimensional heat transfer via both radiation and convection.

Therefore it is reasonable that these results are as they are. The second noticeable feature of the graph is the decreasingly negative slope. It starts out steep and gradually evens out. This is because of the larger temperature difference at its initial higher temperature that drives both the total heat transfer and the heat transfer rates. As more heat is lost, the temperature is decreased and there is therefore a smaller driving temperature difference. As the temperature difference gets smaller, the slope approaches 0—that of a straight line consistent with steady state temperature. The difference between the center and edge is no more than a few degrees at any given time.

The plot for the vertical configuration shows a very similar graph as the horizontal case. However, the functions are slightly different and the actual starting temperature was a few degrees higher at 259°C versus 248°C respectively. However, the total temperature difference for same magnitude of cooling time is also higher by about 4.2 °C, indicating that more heat was transferred from the vertical case than the horizontal.

As shown in table 2, the most heat transferred is via radiation mode in both cases. The vertical configuration passes 406.9W of heat, whereas the horizontal configuration passes only 367W of heat. This is due to the motion created by hot air rising along the face of the vertical plate, while the horizontal plate does not have this effect. Some air will remain stagnant under the plate. The flow is laminar as the Grashof and Prandtl numbers are less than 3×10^{10} for both configurations.

The slopes for both Nu Vs Gr plots are almost identical, regardless of angle and configuration. The straight slope indicates a linear relationship between the Grashof number, which is a ratio of buoyancy forces to viscous forces of natural or free convection, and the Nusselt number which is a ratio of convection to pure conduction heat transfer. It would stand to reason that the slopes and values would vary between the vertical and horizontal plates, however these are almost identical indicating that the ratios in both configurations are roughly the same.

Conclusions and Recommendations

The experiment was excellent practical exposure to heat transfer calculations and approximations. The results were of very good quality, with the errors and discrepancies easily traceable. In the transient conduction part of the experiment, the reconstructed Heisler charts were either linear or had large linear segments when they were scaled correctly, which made derivations of Biot number and heat transfer coefficient easy. The Biot numbers calculated followed very closely with expected trend and varied proportionately with changes in material and geometry. The numbers themselves had errors, and these errors magnified with calculation. The heat transfer coefficients calculated showed large variations (deviations of 16% from the mean). The uncertainties associated with the results are comparatively smaller (0.037 F uncertainty in Theta values and 1 unit of Fourier value) and therefore, other sources were determined to have caused the errors. The sources of the errors were attributed to uncertainties in material properties, variations in the external temperature, reconstruction of Heisler charts, assumptions of one-dimensional heat transfer and infinite geometries in the calculations used, and experimental errors.

The free convection heat transfer results were as expected and closely matched theoretical data from plots and calculations. It was determined that the vertical configuration transferred more heat than the horizontal configuration as the ratio buoyancy forces to viscous forces on the vertical plate were slightly higher, and therefore created a smoother and higher speed laminar flow across the plate. The differences in radiation heat transfer quantities were due to the increased temperature difference driving the system in the two configurations, and can be ignored or minimized in importance relative to the focus of this experiment. Theoretically, for the same time and temperature difference, the radiative portions would be the same unless reflected back by the casing. The difference in convection was about 10W which is significant, but still only a relative small percentage. The vertical configuration transferred more heat at a faster rate than the horizontal configuration due to its added flow lower temperature air over the plate.

It is highly recommended that the external temperature of the water be maintained constant using a PID controller, as this would be far more precise than manually adjusting the temperature to stay constant. The variations in the external water temperature had significant effects on the results. It is also recommended that the thermocouple measuring surface temperature be securely held to the surface by a better method, since a slip of the rubber bands would distort the data.

References

- [1] S. V. Ekkad, revised by M. J. Martin (2008). —Experiment F|| (*ME 4621 Lab Manual for the Transient Heat Transfer Experiment*)
- [2] Pitts and Sissom (1998).—Heat Transfer 2nd Ed|| (*ME 4433 Textbook*)
- [3] M. J. Martin (2008), —Parameter Sheet for Experiments E Through F|| (*Write-up found on moodle*)
- [4] M. J. Martin (2008), —Uncertainty Analysis|| (*Write-up found on moodle*)

Appendices

Appendix I : Planning Sheet

APPENDIX I

LABORATORY PLANNING FORM

DATE: 10/20/08 SECTION: 3 GROUP: 3

EXPERIMENT NUMBER/TITLE: Transient Heat Transfer

GROUP MEMBERS/TASKS: Alejandro Velasquez (Theory, Abstract, Title page, Bibliography) Leader

Cory Mitchel ^{Intro} ~~Theory~~ & Apparatus, Procedure)

Loren Fark [Appendices, Conclusions, Results]

Santhana Balaji [Results, analysis, Uncertainty analysis]

BRIEF STATEMENT OF OBJECTIVE: Measure centerline temperature
as a function of time for the cylinder, sphere & slab of brass and
a slab of steel. Construct the Heissler chart and estimate the
Biot number and value of h based on the Heissler chart.
Compute Nusselt and Grashoff number. ✓

TEST APPARATUS:

Conduction

• Hot Plate ✓

Convection

• Test Plate ✓

• Propane Cylinder

• Gear Pump ✓

• Enclosure ✓

• Water tank ✓

• Heating tube ✓

MEASURED QUANTITIES: • Temperature (water, surface & interior

of specimen), °C & time - Conduction

• Temperature, °C & time - Convection ✓

INSTRUMENTATION: Artificial experimental Control unit

• Thermocouples: Water temp, outside, inside of measured shape. (Conduction)

• Thermocouples (middle & end) - Convection ✓

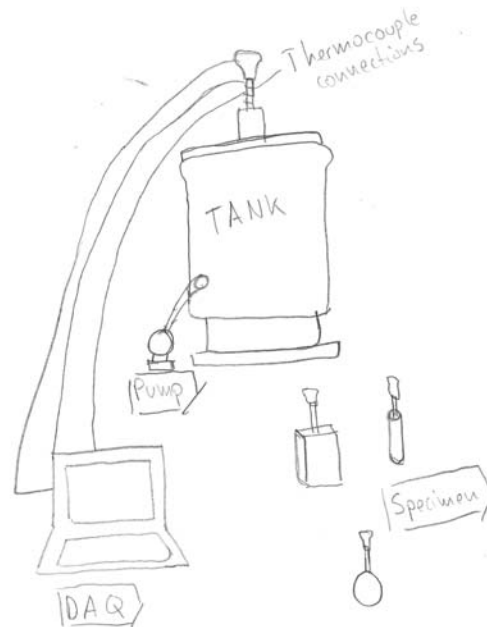
• DAQ units (for both of them)

SKETCH OF APPARATUS AND INSTRUMENTATION SET-UP:

Convection



Conduction



STEP BY STEP LABORATORY PROCEDURE

Convection:

- ✓ Turn Computer on and connect thermocouples.
- ✓ Place aluminum plate facing downward & connect burner to cylinder
- Light burner with lighter
- ✓ Allow thermocouples to reach a 250°C reading
- ✓ Disconnect burner & place outside enclosure
- ✓ Turn the plate to the right orientation & initiate computer, taking data for 1800 seconds
- ✓ Repeat for 90° orientation
- ✓ Shut-down experiment

Conduction:

- ✓ Turn on water heater and attach shape thermocouple toDAQ unit. Attach thermocouple using the rubber band.
- ✓ Let stabilize at room temperature
- ✓ Begin data recording before putting shape in water & insert shape suddenly into water bath
- ✓ Monitor temperature & stop when steady state is achieved.
- ✓ Repeat for different shapes
- ✓ Shut down experiment.

DATA REDUCTION:

Conduction: obtain K_s from $-K_s \frac{\partial T}{\partial x} \big|_{x=0} = h(T - T_{\infty})$

then obtain α value from $\alpha = \frac{K_s}{\rho_s c_p s}$ Calculate Fourier number & plot against θ^* to obtain Heisler chart. Estimate h from

Heisler chart and calculate Biot Number ✓

Convection:

• Compute radiation heat transfer from theory, using temp. values. Estimate convective heat transfer coefficient from

$h = h_r + h_c$ ✓ Compute Nusselt and Grashoff Numbers from formulas.

UNCERTAINTY ANALYSIS:

$$\varepsilon(k_s) = k_s \left[\frac{\varepsilon(T_o)^2}{T_o^2} + \frac{\varepsilon(T_i)^2}{T_i^2} \right]^{1/2}$$

$$\varepsilon(\alpha) = \left[\alpha \frac{\varepsilon(k_s)^2}{k_s^2} \right]^{1/2} ; \quad \varepsilon(\theta^*) = \theta^* \left[\frac{\varepsilon(T_o)^2}{T_o^2} + \frac{\varepsilon(T_i)^2}{T_i^2} \right]^{1/2} \quad \checkmark$$

$$\varepsilon(h_r) = h_r \left[\frac{\varepsilon(T_o)^2}{T_o^2} + \frac{\varepsilon(\Delta T)^2}{T^2} \right]^{1/2} ; \quad \varepsilon(h_c) = h_c \left[\frac{\varepsilon(h_r)^2}{h_r^2} \right]^{1/2}$$

$$\varepsilon(Nu) = Nu \left[\frac{\varepsilon(h_r)^2}{h_r^2} + \frac{\varepsilon(L)^2}{L^2} \right]^{1/2} ; \quad \varepsilon(Gr) = Gr \left[\frac{\varepsilon(T_o)^2}{T_o^2} + \frac{\varepsilon(T_s)^2}{T_s^2} + \frac{\varepsilon(L)^2}{L^2} + \frac{\varepsilon(\theta)^2}{\theta^2} \right]^{1/2}$$

$$\varepsilon(\beta) = \beta \left[\frac{\varepsilon(T)^2}{T^2} \right]^{1/2} \quad \checkmark$$

Appendix II: Vertical Natural Convection Sample Data

Time	Min	Center (°F)	Edge (°F)	Center (K)	Edge (K)	Tinf	Tfilm	β	Gr	Rai	Nu	hbar
14:20:40	0.00	259.94	253.13	533.09	526.28	297.0388889	415.0633	0.002409	152131407.1	106491985	52.83632	6.933900611
14:20:42	0.03	259.33	252.62	532.48	525.77	297.0388889	414.7615	0.002411	151852807	106296965	52.81243	6.930764779
14:20:44	0.07	258.67	252.24	531.82	525.39	297.0388889	414.4296	0.002413	151545998.6	106082199	52.78608	6.927306447
14:20:46	0.10	258.00	251.83	531.15	524.98	297.0388889	414.0925	0.002415	151233786.5	105863651	52.75922	6.922781809
14:20:48	0.13	257.31	251.38	530.46	524.53	297.0388889	413.7496	0.002417	150915727.8	105641009	52.73181	6.920185553
14:20:50	0.17	256.70	250.95	529.85	524.10	297.0388889	413.4428	0.002419	150630753.2	105441527	52.70722	6.916958542
14:20:52	0.20	256.06	250.53	529.21	523.68	297.0388889	413.1264	0.002421	150336370.2	105235459	52.68179	6.913620181
14:20:54	0.23	255.42	250.14	528.57	523.29	297.0388889	412.8031	0.002422	150035101.2	105024571	52.65571	6.910198652
14:20:56	0.27	254.81	249.69	527.96	522.84	297.0388889	412.5005	0.002424	149752647.1	104826863	52.63123	6.906986121
14:20:58	0.30	254.14	249.25	527.29	522.40	297.0388889	412.1663	0.002426	149440266.4	104608186	52.60412	6.903427919
14:21:00	0.33	253.58	248.82	526.73	521.97	297.0388889	411.8833	0.002428	149175393.4	104422775	52.5811	6.900406485
14:21:02	0.37	253.00	248.42	526.15	521.57	297.0388889	411.5943	0.00243	148904434.1	104233104	52.55751	6.897311457
14:21:04	0.40	252.39	247.99	525.54	521.14	297.0388889	411.2895	0.002431	148618298	104032809	52.53257	6.894038484
14:21:06	0.43	251.78	247.57	524.93	520.72	297.0388889	410.9853	0.002433	148332301.9	103832611	52.50761	6.890762387
14:21:08	0.47	251.21	247.15	524.36	520.30	297.0388889	410.6999	0.002435	148063595.7	103644517	52.48412	6.887680026
14:21:10	0.50	250.59	246.70	523.74	519.85	297.0388889	410.3889	0.002437	147770361.3	103439253	52.45845	6.884311509
14:21:12	0.53	250.00	246.28	523.15	519.43	297.0388889	410.0936	0.002438	147491518.4	103244063	52.43401	6.881103666
14:21:14	0.57	249.41	245.81	522.56	518.96	297.0388889	409.8008	0.00244	147214686.7	103050281	52.40971	6.877914446
14:21:16	0.60	248.88	245.45	522.03	518.60	297.0388889	409.5346	0.002442	146962570.5	102873799	52.38755	6.875006048
14:21:18	0.63	248.29	245.06	521.44	518.21	297.0388889	409.2394	0.002444	146682657.5	102677860	52.36291	6.871772601
14:21:20	0.67	247.72	244.57	520.87	517.72	297.0388889	408.953	0.002445	146410750.1	102487525	52.33894	6.868627198
14:21:22	0.70	247.17	244.16	520.32	517.31	297.0388889	408.6781	0.002447	146149356.7	102304550	52.31587	6.865599287
14:21:24	0.73	246.61	243.73	519.76	516.88	297.0388889	408.3969	0.002449	145881608.8	102117126	52.2922	6.862493553
14:21:26	0.77	246.04	243.30	519.19	516.45	297.0388889	408.1155	0.00245	145613253.4	101929277	52.26845	6.859376479
14:21:28	0.80	245.48	242.89	518.63	516.04	297.0388889	407.8363	0.002452	145346677.3	101742674	52.24482	6.856275805
14:21:30	0.83	245.01	242.48	518.16	515.63	297.0388889	407.6009	0.002453	145121637.1	101585146	52.22485	6.853654932
14:21:32	0.87	244.43	241.99	517.58	515.14	297.0388889	407.3079	0.002457	144841216.3	101388851	52.19993	6.850384815
14:21:34	0.90	243.89	241.64	517.04	514.79	297.0388889	407.039	0.002457	144583461.6	101208423	52.177	6.847374827
14:21:36	0.93	243.36	241.22	516.51	514.37	297.0388889	406.7761	0.002458	144331128.8	101031790	52.15451	6.844424254
14:21:38	0.97	242.82	240.79	515.97	513.94	297.0388889	406.502	0.00246	144067698.6	100847389	52.13101	6.841339786
14:21:40	1.00	242.33	240.38	515.48	513.53	297.0388889	406.2602	0.002463	143835016	100684511	52.11022	6.838611817
14:21:42	1.03	241.80	239.99	514.95	513.14	297.0388889	406.0964	0.002463	143580798.6	100506559	52.08748	6.836627587
14:21:44	1.07	241.27	239.52	514.42	512.67	297.0388889	405.7272	0.002465	143321134	100324794	52.06422	6.835275321
14:21:46	1.10	240.76	239.10	513.91	512.25	297.0388889	405.4741	0.002466	143076590.9	100153614	52.04229	6.832697008
14:21:48	1.13	240.24	238.71	513.39	511.86	297.0388889	405.2167	0.002468	142827629.1	99979340	52.01993	6.829762892
14:21:50	1.17	239.73	238.27	512.88	511.42	297.0388889	404.9615	0.002469	142580482.7	99806338	51.99771	6.826845376
14:21:52	1.20	239.26	237.87	512.41	511.02	297.0388889	404.7229	0.002471	142349130.4	99644391	51.97688	6.821112805
14:21:54	1.23	238.72	237.44	511.87	510.59	297.0388889	404.4567	0.002472	142090694.5	99463486	51.95358	6.81805528

Appendix III: Horizontal Natural Convection Sample Data

Time	Min	Center (°C)	Edge (°C)	Center (K)	Edge (K)	T _{inf}	T _{film}	β	Gr	Ra _L	Nubar	hbar
13:37:56	0.00	248.01	246.10	521.1563	519.2518	297.0389	409.0976	0.002444	1465.48057	102583640	52.35105	6.8702161
13:37:58	0.03	247.52	245.59	520.668	518.7372	297.0389	408.8534	0.002446	1463.16084	102421259	52.33059	6.8675311
13:38:00	0.07	246.96	245.02	520.1103	518.1696	297.0389	408.5746	0.002448	1460.50803	102235562	52.30716	6.8644566
13:38:02	0.10	246.36	244.48	519.5076	517.6317	297.0389	408.2732	0.002449	1457.63710	102034597	52.28177	6.8611246
13:38:04	0.13	245.82	244.02	518.9749	517.1689	297.0389	408.0069	0.002451	1455.09607	101856725	52.25927	6.8581714
13:38:06	0.17	245.27	243.52	518.4185	516.6744	297.0389	407.7287	0.002453	1452.43845	101670691	52.2357	6.8550786
13:38:08	0.20	244.74	243.02	517.8876	516.1686	297.0389	407.4632	0.002454	1449.89924	101492947	52.21315	6.8521196
13:38:10	0.23	244.15	242.53	517.3046	515.6802	297.0389	407.1717	0.002456	1447.10704	101297493	52.18832	6.8488612
13:38:12	0.27	243.74	242.08	516.8869	515.2277	297.0389	406.9629	0.002457	1445.10406	101157284	52.17049	6.846521
13:38:14	0.30	243.16	241.58	516.3148	514.7332	297.0389	406.6768	0.002459	1442.35735	100965015	52.14601	6.8433078
13:38:16	0.33	242.70	241.06	515.8459	514.213	297.0389	406.4424	0.00246	1440.10324	100807226	52.12589	6.8406674
13:38:18	0.37	242.17	240.58	515.3193	513.7307	297.0389	406.1791	0.002462	1437.56864	100629805	52.10323	6.8376948
13:38:20	0.40	241.66	240.10	514.8116	513.2539	297.0389	405.9252	0.002464	1435.12190	100458533	52.08154	6.8348215
13:38:22	0.43	241.12	239.68	514.271	512.832	297.0389	405.6549	0.002465	1432.51323	100275926	52.05797	6.8317554
13:38:24	0.47	240.57	239.18	513.7232	512.3252	297.0389	405.381	0.002467	1429.86628	100090639	52.03422	6.8286372
13:38:26	0.50	240.09	238.71	513.2382	511.8645	297.0389	405.1385	0.002468	1427.51978	99926385	52.01313	6.8258706
13:38:28	0.53	239.58	238.22	512.7259	511.3734	297.0389	404.8824	0.00247	1425.03816	99752671	51.99081	6.8229409
13:38:30	0.57	239.04	237.74	512.19	510.8861	297.0389	404.6144	0.002471	1422.43885	99570719	51.9674	6.8198682
13:38:32	0.60	238.53	237.27	511.6803	510.4217	297.0389	404.3596	0.002473	1419.96342	99397439	51.94507	6.816938
13:38:34	0.63	238.11	236.77	511.2555	509.9222	297.0389	404.1472	0.002474	1417.89793	99252855	51.92641	6.8144901
13:38:36	0.67	237.58	236.23	510.7274	509.3752	297.0389	403.8831	0.002476	1415.32715	99072901	51.90317	6.8114396
13:38:38	0.70	237.12	235.79	510.2671	508.9398	297.0389	403.653	0.002477	1413.08367	98915857	51.88286	6.8087742
13:38:40	0.73	236.57	235.27	509.7215	508.4197	297.0389	403.3802	0.002479	1410.42113	98729479	51.85872	6.8056067
13:38:42	0.77	236.14	234.82	509.2888	507.974	297.0389	403.1638	0.00248	1408.30698	98581489	51.83953	6.8030884
13:38:44	0.80	235.60	234.36	508.7489	507.5051	297.0389	402.8939	0.002482	1405.66588	98396611	51.81553	6.7999384
13:38:46	0.83	235.17	233.87	508.3156	507.0175	297.0389	402.6772	0.002483	1403.54368	98248058	51.77355	6.7974041
13:38:48	0.87	234.66	233.38	507.8082	506.5275	297.0389	402.4235	0.002485	1401.05566	98073896	51.73922	6.7944293
13:38:50	0.90	234.22	232.88	507.3674	506.0344	297.0389	402.2031	0.002486	1398.89165	97922416	51.75381	6.7918387
13:38:52	0.93	233.75	232.39	506.8954	505.5376	297.0389	401.9671	0.002488	1396.57185	97760030	51.73262	6.7890582
13:38:54	0.97	233.26	232.00	506.4115	505.152	297.0389	401.7252	0.002489	1394.19074	97593352	51.71085	6.7862006
13:38:56	1.00	232.85	231.53	505.9985	504.6786	297.0389	401.5187	0.002491	1392.15623	97450936	51.69222	6.7837561
13:38:58	1.03	232.36	231.09	505.5104	504.2416	297.0389	401.2746	0.002492	1389.74906	97282434	51.67016	6.7808604
13:39:00	1.07	231.88	230.60	505.0252	503.7538	297.0389	401.032	0.002494	1387.35329	97114731	51.64817	6.7779746
13:39:02	1.10	231.42	230.17	504.5686	503.3153	297.0389	400.8037	0.002495	1385.09609	96956727	51.62742	6.7752523
13:39:04	1.13	230.95	229.70	504.0972	502.8501	297.0389	400.568	0.002496	1382.76303	96793412	51.60556	6.7724351

Appendix IV: Steel Slab Sample Data

Time	ms	Time	Fo	Water T. °C	Surface T. °C	Theta	Center T. °C
14:00:16	0			82.23	27.88		28.37
14:00:16	500			82.24	27.79		28.30
14:00:17	0			82.43	27.95		28.33
14:00:18	500	0.0	0.0	82.30	27.92	1.00	28.51
14:00:18	0	0.5	0.0	82.45	30.32	1.00	28.31
14:00:19	500	1.0	0.1	82.49	57.97	1.00	28.29
14:00:19	0	1.5	0.1	82.52	67.76	1.00	28.31
14:00:20	500	2.0	0.1	82.54	70.77	1.00	28.47
14:00:20	0	2.5	0.2	82.42	70.66	1.00	28.64
14:00:21	500	3.0	0.2	82.17	70.22	0.99	29.09
14:00:21	0	3.5	0.2	82.15	70.86	0.98	29.77
14:00:21	500	4.0	0.3	81.83	70.55	0.96	30.55
14:00:22	0	4.5	0.3	81.91	70.36	0.94	31.50
14:00:22	500	5.0	0.3	81.70	69.81	0.92	32.58
14:00:23	0	5.5	0.4	81.52	69.43	0.90	33.66
14:00:23	500	6.0	0.4	81.45	69.56	0.88	34.65
14:00:24	0	6.5	0.5	81.28	69.64	0.86	35.71
14:00:24	500	7.0	0.5	81.11	69.45	0.85	36.63
14:00:25	0	7.5	0.5	81.15	69.48	0.83	37.63
14:00:26	500	8.0	0.6	81.13	69.96	0.81	38.55
14:00:26	0	8.5	0.6	80.96	70.30	0.79	39.44
14:00:27	500	9.0	0.6	81.07	70.78	0.77	40.36
14:00:27	0	9.5	0.7	80.97	71.61	0.76	41.20
14:00:28	500	10.0	0.7	81.07	71.49	0.74	41.99
14:00:28	0	10.5	0.7	80.96	72.02	0.73	42.78
14:00:28	500	11.0	0.8	80.99	72.32	0.71	43.55
14:00:29	0	11.5	0.8	81.03	72.14	0.70	44.34
14:00:29	500	12.0	0.8	80.93	72.08	0.68	45.03
14:00:30	0	12.5	0.9	80.83	72.06	0.67	45.73
14:00:30	500	13.0	0.9	81.00	72.06	0.66	46.41
14:00:31	0	13.5	0.9	80.92	71.86	0.65	47.10
14:00:31	500	14.0	1.0	80.97	71.77	0.63	47.71
14:00:32	0	14.5	1.0	80.87	71.98	0.62	48.32
14:00:33	500	15.0	1.0	80.85	72.39	0.61	48.90
14:00:33	0	15.5	1.1	80.90	72.44	0.60	49.52
14:00:34	500	16.0	1.1	80.89	72.54	0.59	50.04
14:00:34	0	16.5	1.1	80.75	72.81	0.58	50.62
14:00:35	500	17.0	1.2	80.75	73.36	0.57	51.21
14:00:35	0	17.5	1.2	80.80	73.45	0.55	51.81
14:00:36	500	18.0	1.3	80.95	73.42	0.55	52.36
14:00:36	0	18.5	1.3	80.89	73.64	0.53	53.01
14:00:36	500	19.0	1.3	80.93	73.95	0.52	53.56
14:00:37	0	19.5	1.4	80.90	74.42	0.51	54.09
14:00:37	500	20.0	1.4	80.93	74.56	0.50	54.65
14:00:38	0	20.5	1.4	81.01	74.59	0.49	55.19
14:00:38	500	21.0	1.5	80.91	74.51	0.48	55.67
14:00:39	0	21.5	1.5	80.98	74.48	0.47	56.17
14:00:39	500	22.0	1.5	80.90	74.58	0.46	56.58
14:00:40	0	22.5	1.6	80.93	74.54	0.46	57.05
14:00:41	500	23.0	1.6	80.90	74.65	0.45	57.46

Appendix V: Brass Slab Sample Data

Time	ms	Time	Time_Fo	Fo	Water T. ~C	Surface T. ~C	Theta_0/Theta_i	Center T. ~C
13:48:09	0	0.0			80.54	27.94	1.00	27.13
13:48:09	500	0.5			80.53	28.29	1.00	27.16
13:48:10	0	1.0			80.52	28.41	1.00	27.16
13:48:10	500	1.5			80.57	28.36	1.00	27.20
13:48:11	0	2.0			80.61	28.09	1.00	27.21
13:48:11	500	2.5			80.59	28.16	1.00	27.18
13:48:12	0	3.0			80.60	28.36	1.00	27.23
13:48:13	500	3.5			80.59	28.54	1.00	27.23
13:48:13	0	4.0			80.56	28.66	1.00	27.23
13:48:14	500	4.5			80.59	28.98	1.00	27.26
13:48:14	0	5.0			80.56	28.94	1.00	27.28
13:48:15	500	5.5			80.58	29.06	1.00	27.29
13:48:15	0	6.0			80.58	29.19	1.00	27.29
13:48:15	500	6.5			80.58	29.35	1.00	27.30
13:48:16	0	7.0			80.58	29.56	1.00	27.34
13:48:16	500	7.5			80.56	29.63	1.00	27.40
13:48:17	0	8.0			80.58	29.58	1.00	27.37
13:48:17	500	8.5			80.57	29.49	0.99	27.41
13:48:18	0	9.0			80.61	29.41	0.99	27.41
13:48:18	500	9.5			80.61	29.26	0.99	27.46
13:48:19	0	10.0			80.61	29.36	0.99	27.49
13:48:20	500	10.5			80.67	29.37	0.99	27.52
13:48:20	0	11.0			80.63	29.43	0.99	27.55
13:48:21	500	11.5			80.63	29.61	0.99	27.58
13:48:21	0	12.0			80.60	29.65	0.99	27.60
13:48:22	500	12.5			80.60	29.72	0.99	27.63
13:48:22	0	13.0	0.0	0.0	80.61	29.83	1.00	27.64
13:48:23	500	13.5	0.5	0.3	80.62	37.01	1.00	27.68
13:48:23	0	14.0	1.0	0.6	80.61	59.40	0.99	27.92
13:48:23	500	14.5	1.5	0.9	80.62	63.51	0.99	28.31
13:48:24	0	15.0	2.0	1.2	80.61	65.42	0.96	29.52
13:48:24	500	15.5	2.5	1.5	80.30	64.77	0.94	30.86
13:48:25	0	16.0	3.0	1.8	80.42	64.33	0.91	32.21
13:48:25	500	16.5	3.5	2.1	80.38	64.27	0.89	33.49
13:48:26	0	17.0	4.0	2.4	79.96	64.37	0.86	34.72
13:48:26	500	17.5	4.5	2.7	79.93	65.73	0.84	35.98
13:48:27	0	18.0	5.0	3.0	80.10	65.48	0.81	37.40
13:48:28	500	18.5	5.5	3.3	79.92	68.29	0.79	38.59
13:48:28	0	19.0	6.0	3.6	80.00	71.67	0.77	39.85
13:48:29	500	19.5	6.5	3.9	79.97	73.60	0.74	41.00
13:48:29	0	20.0	7.0	4.2	79.86	74.81	0.72	42.10
13:48:30	500	20.5	7.5	4.5	79.76	71.77	0.70	43.19
13:48:30	0	21.0	8.0	4.8	79.81	68.99	0.68	44.24
13:48:30	500	21.5	8.5	5.1	79.82	67.16	0.66	45.18
13:48:31	0	22.0	9.0	5.4	79.60	67.32	0.64	46.32
13:48:31	500	22.5	9.5	5.7	79.64	68.97	0.62	47.30
13:48:32	0	23.0	10.0	6.0	79.57	69.40	0.60	48.31
13:48:32	500	23.5	10.5	6.3	79.58	70.11	0.58	49.35
13:48:33	0	24.0	11.0	6.6	79.56	70.35	0.56	50.41
13:48:33	500	24.5	11.5	6.9	79.29	71.36	0.54	51.65

Appendix VI: Brass Sphere Sample Data

Time	ms	Time	Time_Fo	Fo	Water T. °C	Surface T. °C	Theta_0/TI Center T. °C
14:21:24	0	0.0			79.34	28.74	29.41
14:21:24	500	0.5			79.38	28.72	29.36
14:21:25	0	1.0			79.41	28.72	29.40
14:21:25	500	1.5			79.42	28.77	29.41
14:21:26	0	2.0			79.45	28.79	29.40
14:21:27	500	2.5			79.42	28.86	29.39
14:21:27	0	3.0	0.0	0.0	79.51	29.76	1.00 29.31
14:21:28	500	3.5	0.5	0.0	79.49	52.58	1.00 29.40
14:21:28	0	4.0	1.0	0.1	79.47	64.06	0.99 29.65
14:21:29	500	4.5	1.5	0.1	79.53	66.99	0.98 30.38
14:21:29	0	5.0	2.0	0.1	79.48	65.90	0.96 31.52
14:21:29	500	5.5	2.5	0.2	79.51	66.93	0.92 33.27
14:21:30	0	6.0	3.0	0.2	79.47	68.27	0.89 34.90
14:21:30	500	6.5	3.5	0.2	79.39	68.61	0.85 36.72
14:21:31	0	7.0	4.0	0.3	79.47	68.54	0.82 38.39
14:21:31	500	7.5	4.5	0.3	79.41	68.08	0.79 39.89
14:21:32	0	8.0	5.0	0.3	79.29	68.82	0.76 41.23
14:21:32	500	8.5	5.5	0.4	79.25	68.53	0.74 42.45
14:21:33	0	9.0	6.0	0.4	79.23	68.63	0.71 43.67
14:21:34	500	9.5	6.5	0.4	79.19	69.32	0.69 44.78
14:21:34	0	10.0	7.0	0.5	79.24	70.03	0.67 45.86
14:21:35	500	10.5	7.5	0.5	79.26	70.69	0.65 46.88
14:21:35	0	11.0	8.0	0.5	79.13	70.60	0.63 47.80
14:21:36	500	11.5	8.5	0.6	79.10	70.01	0.61 48.71
14:21:36	0	12.0	9.0	0.6	79.05	70.73	0.59 49.62
14:21:37	500	12.5	9.5	0.6	79.02	70.61	0.58 50.43
14:21:37	0	13.0	10.0	0.7	79.02	70.18	0.56 51.26
14:21:37	500	13.5	10.5	0.7	78.87	69.89	0.54 52.07
14:21:38	0	14.0	11.0	0.7	78.95	70.55	0.53 52.87
14:21:38	500	14.5	11.5	0.8	78.95	70.62	0.51 53.67
14:21:39	0	15.0	12.0	0.8	78.94	71.50	0.49 54.43
14:21:39	500	15.5	12.5	0.8	78.98	72.59	0.48 55.19
14:21:40	0	16.0	13.0	0.9	78.93	72.50	0.46 55.86
14:21:40	500	16.5	13.5	0.9	78.94	72.30	0.45 56.55
14:21:41	0	17.0	14.0	0.9	78.90	72.04	0.44 57.21
14:21:42	500	17.5	14.5	1.0	78.86	72.06	0.43 57.80
14:21:42	0	18.0	15.0	1.0	78.90	72.52	0.41 58.41
14:21:43	500	18.5	15.5	1.0	78.84	72.66	0.40 58.96
14:21:43	0	19.0	16.0	1.1	78.67	73.04	0.39 59.59
14:21:44	500	19.5	16.5	1.1	78.81	73.33	0.38 60.15
14:21:44	0	20.0	17.0	1.1	78.83	73.01	0.37 60.75
14:21:44	500	20.5	17.5	1.2	78.91	73.08	0.36 61.27
14:21:45	0	21.0	18.0	1.2	78.78	73.04	0.34 61.72
14:21:45	500	21.5	18.5	1.2	78.82	73.43	0.34 62.18
14:21:46	0	22.0	19.0	1.3	78.76	73.64	0.33 62.68
14:21:46	500	22.5	19.5	1.3	78.78	74.25	0.32 63.13
14:21:47	0	23.0	20.0	1.3	78.83	74.72	0.31 63.65
14:21:47	500	23.5	20.5	1.4	78.86	74.85	0.30 64.11
14:21:48	0	24.0	21.0	1.4	78.87	74.90	0.29 64.53
14:21:49	500	24.5	21.5	1.4	78.81	74.77	0.28 64.96

Appendix VII: Small Brass Cylinder Sample Data

Time	ms	Time	Time_Fo	Fo	Water T. ~C	Surface T. ~C	Theta_0/Th Center T. ~C
14:05:18	0	0.0			81.66	26.18	1.00
14:05:18	500	0.5			81.71	26.16	1.00
14:05:19	0	1.0			81.82	26.18	1.00
14:05:19	500	1.5			81.79	26.12	1.00
14:05:20	0	2.0			81.89	26.19	1.00
14:05:20	500	2.5			81.86	26.41	1.00
14:05:21	0	3.0			81.39	26.43	0.99
14:05:21	500	3.5			81.96	26.83	1.01
14:05:22	0	4.0	0.0	0.0	81.89	29.14	1.00
14:05:23	500	4.5	0.5	0.2	81.78	57.29	1.00
14:05:23	0	5.0	1.0	0.3	81.75	65.07	0.97
14:05:24	500	5.5	1.5	0.5	81.81	69.80	0.91
14:05:24	0	6.0	2.0	0.7	81.83	70.30	0.85
14:05:25	500	6.5	2.5	0.8	81.79	71.58	0.80
14:05:25	0	7.0	3.0	1.0	81.77	72.31	0.75
14:05:25	500	7.5	3.5	1.2	81.74	71.95	0.71
14:05:26	0	8.0	4.0	1.4	81.76	72.45	0.67
14:05:26	500	8.5	4.5	1.5	81.70	73.01	0.63
14:05:27	0	9.0	5.0	1.7	81.49	72.83	0.60
14:05:27	500	9.5	5.5	1.9	81.35	73.56	0.56
14:05:28	0	10.0	6.0	2.0	81.30	73.09	0.53
14:05:28	500	10.5	6.5	2.2	81.23	73.35	0.50
14:05:29	0	11.0	7.0	2.4	81.18	74.29	0.47
14:05:30	500	11.5	7.5	2.5	81.25	74.65	0.45
14:05:30	0	12.0	8.0	2.7	81.25	75.10	0.42
14:05:31	500	12.5	8.5	2.9	81.22	74.71	0.40
14:05:31	0	13.0	9.0	3.1	81.14	75.30	0.38
14:05:32	500	13.5	9.5	3.2	81.03	75.55	0.36
14:05:32	0	14.0	10.0	3.4	81.10	75.59	0.34
14:05:33	500	14.5	10.5	3.6	81.09	75.83	0.32
14:05:33	0	15.0	11.0	3.7	81.05	76.18	0.30
14:05:33	500	15.5	11.5	3.9	81.03	76.36	0.28
14:05:34	0	16.0	12.0	4.1	80.96	76.36	0.27
14:05:34	500	16.5	12.5	4.2	81.01	76.55	0.25
14:05:35	0	17.0	13.0	4.4	80.94	77.04	0.24
14:05:35	500	17.5	13.5	4.6	80.93	77.40	0.22
14:05:36	0	18.0	14.0	4.7	80.98	77.43	0.21
14:05:37	500	18.5	14.5	4.9	80.92	77.65	0.20
14:05:37	0	19.0	15.0	5.1	80.95	77.85	0.19
14:05:38	500	19.5	15.5	5.3	80.96	78.12	0.18
14:05:38	0	20.0	16.0	5.4	80.96	78.25	0.17
14:05:39	500	20.5	16.5	5.6	81.02	78.25	0.16
14:05:39	0	21.0	17.0	5.8	80.92	78.44	0.15
14:05:40	500	21.5	17.5	5.9	81.01	78.42	0.15
14:05:40	0	22.0	18.0	6.1	81.02	78.61	0.14
14:05:40	500	22.5	18.5	6.3	81.01	78.77	0.13
14:05:41	0	23.0	19.0	6.4	81.01	78.91	0.12
14:05:41	500	23.5	19.5	6.6	80.96	79.04	0.12
14:05:42	0	24.0	20.0	6.8	81.04	79.22	0.11
14:05:42	500	24.5	20.5	6.9	81.03	79.28	0.11

Appendix VIII: Large Brass Cylinder Sample Data

Time	ms	Time	Time_Fo	Fo	Water T. ~C	Surface T. ~C	Theta_0/Ti Center T. ~C
14:09:39	0				81.06	27.71	28.09
14:09:39	500				81.11	27.73	28.08
14:09:40	0				81.18	27.73	28.00
14:09:40	500				81.09	27.67	28.00
14:09:41	0				81.09	27.92	28.04
14:09:42	500				81.07	28.13	28.18
14:09:42	0				81.19	28.16	27.96
14:09:43	500				81.15	28.22	28.09
14:09:43	0				81.15	28.34	28.05
14:09:44	500				81.13	28.21	28.14
14:09:44	0				81.05	28.21	28.14
14:09:45	500				81.07	28.18	28.13
14:09:45	0				81.12	28.07	27.88
14:09:45	500				81.26	28.01	27.98
14:09:46	0				81.06	28.02	28.15
14:09:46	500				81.07	27.98	28.09
14:09:47	0				81.08	27.98	28.10
14:09:47	500		0.0	0.00	81.02	28.08	1.00 28.02
14:09:48	0		0.5	0.08	81.09	52.88	1.00 28.02
14:09:49	500		1.0	0.15	81.08	63.91	1.00 28.16
14:09:49	0		1.5	0.23	81.17	67.24	0.99 28.72
14:09:50	500		2.0	0.30	79.91	67.59	0.97 29.83
14:09:50	0		2.5	0.38	80.51	70.31	0.94 30.93
14:09:51	500		3.0	0.45	80.31	70.77	0.92 32.39
14:09:51	0		3.5	0.53	80.68	71.63	0.89 33.87
14:09:52	500		4.0	0.60	79.82	71.65	0.86 35.29
14:09:52	0		4.5	0.68	80.07	72.84	0.83 36.82
14:09:52	500		5.0	0.75	80.46	71.94	0.80 38.36
14:09:53	0		5.5	0.83	80.55	71.60	0.77 39.87
14:09:53	500		6.0	0.90	80.53	70.90	0.75 41.33
14:09:54	0		6.5	0.98	80.34	70.03	0.72 42.56
14:09:54	500		7.0	1.05	80.39	69.97	0.69 44.01
14:09:55	0		7.5	1.13	80.22	70.27	0.67 45.20
14:09:55	500		8.0	1.21	80.17	70.09	0.65 46.43
14:09:56	0		8.5	1.28	80.06	69.65	0.63 47.53
14:09:57	500		9.0	1.36	80.00	71.29	0.60 48.66
14:09:57	0		9.5	1.43	79.93	71.66	0.58 49.74
14:09:58	500		10.0	1.51	79.87	71.32	0.56 50.74
14:09:58	0		10.5	1.58	79.94	71.11	0.54 51.80
14:09:59	500		11.0	1.66	79.90	71.50	0.52 52.78
14:09:59	0		11.5	1.73	79.92	71.94	0.50 53.77
0.590278	500		12.0	1.81	79.93	72.07	0.49 54.67
14:10:00	0		12.5	1.88	79.87	72.55	0.47 55.51
14:10:00	500		13.0	1.96	79.83	72.67	0.45 56.33
14:10:01	0		13.5	2.03	79.84	73.50	0.44 57.18
14:10:01	500		14.0	2.11	79.63	73.61	0.42 57.97
14:10:02	0		14.5	2.18	79.81	73.76	0.41 58.77
14:10:02	500		15.0	2.26	79.89	73.78	0.39 59.52
14:10:03	0		15.5	2.34	79.84	73.95	0.38 60.19
14:10:04	500		16.0	2.41	79.77	73.87	0.37 60.79

Appendix IX: Sample Calculations